Eur. Phys. J. D **23**, 291–297 (2003)
DOI: 10.1140/epjd/e2003-00057-1

THE EUROPEAN PHYSICAL JOURNAL D

Feedback controlled periodic states for different kinds of photorefractive nonlinear response

B.I. Sturman[1], A.S. Gorkunova[2,a], and K.H. Ringhofer[2,†]

[1] International Institute for Nonlinear Studies, Koptyug Ave. 1, 630090 Novosibirsk, Russia
[2] Department of Physics, University of Osnabrück, 49069 Osnabrück, Germany

Received 16 July 2002 / Received in final form 29 October 2002
Published online 4 March 2003 –

Abstract. We investigate analytically and numerically the influence of the type of the photorefractive nonlinear response on the periodic states (attractors) which occur during feedback controlled 2W-coupling and correspond to almost 100% diffraction efficiency of the dynamic index grating. In addition to the case of the local response typical, for example, for $LiNbO_3$ crystals we consider the cases of nonlocal (diffusive) response ($BaTiO_3$, SBN) and resonant response (DC-biased BSO, BTO, and BGO crystals). It is shown that the conditions for the transition to the periodic states and their apparent characteristics are strongly different for the two limiting cases above.

PACS. 42.65.Hw Phase conjugation; photorefractive and Kerr effects – 42.40.Pa Volume holograms – 42.65.Sf Dynamics of nonlinear optical systems; optical instabilities, optical chaos and complexity, and optical spatio-temporal dynamics

1 Introduction

The photorefractive feedback controlled 2W-coupling has been under experimental and theoretical study during the last decade [1–8]. It was found first for $LiNbO_3$ crystals [2–5] that an electronic feedback loop, governing the input phase of the signal beam, produces dramatic changes in the characteristics of 2W-mixing. In particular, this feedback has allowed the suppression of light-induced scattering, the stabilization of the input light fringes, and the 100% diffraction efficiency of the recorded index grating.

The first theoretical formulation of the feedback problem was proposed in [6]. It adapted the idea of a $\pi/2$ phase shift between the diffracted and transmitted components of the signal (S) beam at the crystal output [2]. Numerical simulations of the derived equations have shown [6] that the nonlinear system approaches quickly a state where the dynamic index grating is fully diffractive and the formulated (ideal) $\pi/2$ feedback conditions fail. This ideal model is therefore applicable only to the initial stage of development.

The breakthrough in the understanding of the feedback operation was made in [7,8]. It was shown that the inertia of the feedback loop is the key element of the permanent operation of the whole system. Unless the transmitted component of the signal beam is very close to zero, this inertia is of minor importance. At this point, the diffraction efficiency of the dynamic index grating, η, approaches unity. Close to unity the output phase difference between the diffracted and transmitted components of the S-beam becomes non-physical. The feedback loop fails to adjust this phase difference to $\pi/2$ and the system moves by inertia. At this stage, the diffraction efficiency is decreasing which brings the feedback into play again to increase η.

In this situation we have instead of steady-states (typical of 2W-coupling), certain periodic states (attractors). For an attractor, the diffractivity η oscillates close to unity, the input phase of the S-beam, $\varphi_s(t)$, possesses both a linear trend and a periodically oscillating component, and the point on the complex plane mapping the output amplitude of a wave testing the index grating is moving along a periodic orbit. This behavior is easily recognizable in experiment [7,8].

An essential feature of the current theoretical studies of the feedback-controlled 2W-coupling is the dominance of numerical methods over analytical ones. Analytical considerations are involved mostly for derivation of the initial nonlinear equations and some auxiliary functions. Even for the ideal inertia-free model there is still no general proof of the assertion regarding the maximization of η by the feedback. The belief in this assertion is based on numerous experiments and numerical calculations.

Until now, theoretical and experimental studies of the periodic states were concerned with the case of the so-called local photorefractive response, which is typical for example for $LiNbO_3$ crystals. There are, however, two other important types of photorefractive nonlinear

[a] e-mail: mgorkoun@uni-osnabrueck.de
† This author dead in December 26, 2002.

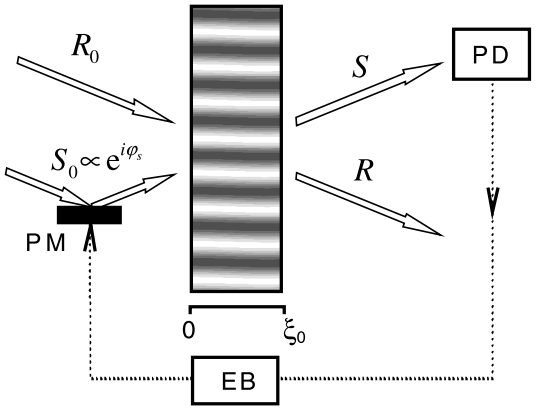

Fig. 1. Schematic of a feedback experiment; PM is a piezo-mirror, PD is a photo-diode, and EB is an electronic block.

response. The first of them is the nonlocal (diffusive) response [9] which corresponds to the diffusive charge transport mechanism in slow photorefractive ferroelectrics like $BaTiO_3$ and SBN. The second one can be called the resonant response. It is typical of fast photorefractive crystals (the sillenites, BSO, BTO, and BGO, the semiconductors GaAs, CdTe, etc.) placed in an electric DC-field [9,10]. The distinctive feature of this response is that it can be strongly enhanced under the condition of resonance between an eigenfrequency of the material and the frequency of an external driving force [11]. Here one can expect new features in behavior of the feedback controlled 2W-coupling.

The aim of this paper is an analysis of the periodic states governed by the feedback for the cases of nonlocal and resonant response. While the specific results of this study are obtained numerically, some important judgments on the expected region of the variable parameters relevant to the periodic states are deduced analytically on the basis of the theory of fast phase modulation [12,13].

2 Initial equations

A schematic diagram of a feedback experiment is shown in Figure 1. Two light beams, the reference (R) and signal (S) are incident on the crystal. The input phase of the S-beam, φ_s, is governed, *via* an electronic loop, by output optical parameters, see [6,7] and references therein for more details. The input phase of the R-beam is assumed to be constant. The initial set of dimensionless equations for the beam amplitudes R and S and the grating amplitude E is not different from that used in [8]; we cast them in the form

$$\partial_\xi R = \mathrm{i}ES \tag{1}$$

$$\partial_\xi S = \mathrm{i}E^*R \tag{2}$$

$$\left(\mathrm{e}^{\mathrm{i}\delta}\,\partial_\tau + 1\right) E = \mathrm{e}^{\mathrm{i}\theta}\,R\,S^* \tag{3}$$

where ξ and τ are the dimensionless coordinate and time, while θ and δ are the characteristic phases that specify the type of the nonlinear response, see also below. The amplitudes R and S are normalized in such a way that the integral of motion $|R|^2 + |S|^2 = 1$.

The feedback condition supplementing the set (1–3) has the form of an ordinary first-order differential equation for the input phase φ_s [7,8]:

$$\dot{\varphi}_s = -\frac{1}{\tau_\mathrm{f}}\,|R_0 S_0|\,\sqrt{\eta(1-\eta)}\,\cos\Phi_s. \tag{4}$$

Here R_0 and S_0 are the input values of R and S, τ_f is the dimensionless response time of the electronic feedback loop, η the diffraction efficiency, and Φ_s the phase difference between the diffracted and transmitted components of the signal beam at the crystal output ($\xi = \xi_0$). This phase difference can be expressed algebraically (and nonlinearly) through the input and output values of R and S [8]. As long as the factor $\eta(1-\eta)$ is far from zero, Φ_s relaxes very quickly (in a time $\sim \tau_\mathrm{f} \ll 1$) to the value $\pi/2$, *i.e.*, the ideal feedback condition takes place. As soon as $\eta(1-\eta)$ approaches zero, the phase φ_s cannot react to the feedback signal and the phase difference Φ_s deflects strongly from the ideal $\pi/2$ value.

The dimensionless coordinate ξ and time τ can indeed be expressed through the propagation coordinate x and the real time t. The form of this connection depends, however, on the type of the nonlinear response. The case of the local nonlinear response has been considered in [6–8]. Two other limiting cases are of interest in the present study.

The nonlocal response. This case corresponds to $\delta = 0$ and $\theta = \pm\pi/2$. Physically, both the signs are equivalent (in what follows we restrict ourselves to the sign + for convenience). The index distribution formed by a static light pattern is proportional to the intensity gradient, $\tau = t/t_\mathrm{d}$ and $\xi = x\,(\pi n^3 r E_\mathrm{D}/\lambda)$, where t_d is the Maxwell relaxation time, n the non-perturbed refractive index, r the relevant electro-optic coefficient, λ the wave length, and E_D the characteristic diffusion field which depends on the temperature and the period of the light interference pattern Λ. Typically, the diffusion field is as large as a few kV/cm in 2W-coupling experiments. No external electric field is expected to be applied to the crystal.

The resonant response. In this case we have $\theta = 0$, and $0 < (\pi/2) - \delta \ll 1$. To make the physical situation in question more clear, we transform equation (3) into

$$(\partial_\tau - \mathrm{i} + \cos\delta)\,E = -\mathrm{i}\,R\,S^*. \tag{5}$$

When the right-hand side equals zero, this equation describes a weakly damped oscillator and in our case it corresponds to a weakly damped space-charge wave of period of Λ [11]. Correspondingly, we identify $\cos\delta$ with the inverse of the quality factor of this wave, Q^{-1}, and the dimensionless time τ with the product $\omega_0 t$, where ω_0 is the eigenfrequency of the space-charge wave. The quality factor Q is an even function of the applied DC-field E_0; in crystals of the sillenite family (BSO, BTO, and BGO) and for typical experimental conditions it is as large as (5–7). Correspondingly, we estimate $\cos\delta = 0.15$–0.2. The frequency ω_0 is an odd function of E_0. Switching from E_0 to $-E_0$ means changing sign before the imaginary unit in the

left-hand side of equation (5). Both these cases are physically equivalent. To obtain the relation between ξ and x one has to replace $E_{\rm D}$ with $|E_0|$ in the expression for ξ given in the previous paragraph.

The specific feature of the resonant case is a considerable increase of the grating amplitude E when the right-hand side of equation (5) (*i.e.*, the effective driving force) is at resonance with the eigen mode. If the feedback is able to find this resonance, one can expect a decrease of the dimensional crystal thickness ξ_0, necessary to achieve a 100% diffraction efficiency.

3 Existence curves

On the basis of previous experience with the local response [6–8], the operation mode of the feedback can qualitatively be explained as follows. The ideal feedback always tends to maximize η. For thin crystals (*i.e.*, a sufficiently small ξ_0) the value of $\eta_{\max}$ is indeed less than unity. It corresponds to a steady-state for 2W-mixing and the only fitting parameter in "possession" of the feedback is the frequency detuning Ω between the R- and S-beams. This detuning is accomplished by the corresponding linear change of the feedback-controlled input phase, $\varphi_s = \Omega\tau$. The value of $\eta_{\max}$ and the corresponding detuning $\Omega_{\max}$ are functions of the thickness ξ_0 and the input intensity ratio $\beta = |S_0|^2/|R_0|^2$. The form of these functions depends on the type of the nonlinear response. With increasing ξ_0, the value of $\eta_{\max}$ reaches unity. At this threshold we still have no periodic state but merely a steady state.

Some simple and important judgments concerning the possibility to adjust η to unity in a steady state can be made from general considerations. To get $\eta = 1$, one has to adjust to zero both the real and imaginary parts of the transmitted component of the S-beam (or R-beam). Thus we have two constraints on the variable parameters ξ_0, β, and Ω which means that $\xi_0 = \xi_{\rm th}(\beta)$ and $\Omega = \Omega_{\rm th}(\beta)$ are certain functions of the input beam ratio. For each value of β there is therefore a single value of ξ_0 compatible with the condition $\eta = 1$. The next judgment which follows from this consideration of the steady state is also important: for $\xi_0 > \xi_{\rm th}$ the efficiency η drops in value and it cannot be adjusted to unity by changing Ω in the general case.

The role of the feedback in the case of an excessive crystal thickness $[\xi_0 > \xi_{\rm th}(\beta)]$ is in the introduction of an additional periodic phase modulation into $\varphi_s(\tau)$ to compensate the overshoot. If this periodic modulation is fast (which is the case when the feedback response time $\tau_{\rm f}$ is sufficiently short) its effect on the characteristics of 2W-coupling can be described by the only new parameter ε defined by the relation

$$\varepsilon = |\langle \exp(\mathrm{i}\varphi_p)\rangle| \,, \tag{6}$$

where the brackets mean averaging over the oscillation period $T \ll 1$ and $\varphi_p(\tau)$ is the T-periodic component of $\varphi_s(\tau)$. With no modulation we have $\varepsilon = 1$, whereas for a strong modulation $\varepsilon \ll 1$. The presence of this new variable parameter allows the feedback to adjust η to unity for $\xi_0 > \xi_{\rm th}$. The specific form of the periodic phase modulation (the form of the function $\varphi_p(\tau)$) is beyond qualitative and analytical considerations.

As follows from the above analysis, a periodic state with $\eta \simeq 1$ can exist only when the dimensional crystal thickness ξ_0 exceeds the threshold value $\xi_{\rm th}(\beta)$. To find this function, it is sufficient to solve the set (1–3) in steady state to find η and to meet the condition $\eta = 1$. The final result can be easily extracted from equations (30–40) of [13] by setting $\varepsilon = 1$. We apply it below to the cases of the local, nonlocal, and resonant response to separate the regions where the periodic states with $\eta = 1$ can and cannot exist.

The local response. Here we set $\theta = 0$, $\delta = 0$. The corresponding threshold values $\xi_{\rm th}$ and $\Omega_{\rm th}$ are

$$\xi_{\rm th} = \pi + \frac{1}{\pi}\,\ln^2\beta\,, \qquad \Omega_{\rm th} = \pm\frac{1}{\pi}\,\ln\beta. \tag{7}$$

According to these relations, the minimum threshold thickness, $\xi_{\rm th}^{\min} = \pi$, corresponds to $\beta = 1$ and $\Omega_{\rm th} = 0$. Furthermore we have $\xi_{\rm th}(\beta) = \xi_{\rm th}(1/\beta)$, *i.e.*, the threshold thickness is symmetric to interchange of the pump intensities. The detuning $\Omega_{\rm th}$ is an odd function of the pump difference $|S_0|^2 - |R_0|^2 \equiv (\beta-1)/(\beta+1)$. The corresponding plots are presented in Figure 2. In the case of the local response, they are in full agreement with the numerical data of [7,8] relating to the periodic states.

The nonlocal response, $\theta = \pi/2$, $\delta = 0$. Here we have at the threshold:

$$\xi_{\rm th} = -\left(\ln\beta + \frac{\pi^2}{\ln\beta}\right), \qquad \Omega_{\rm th} = \pm\frac{\pi}{\ln\beta}. \tag{8}$$

The minimum dimensionless threshold thickness $\xi_{\rm th}^{\min}$ is here 2π and it corresponds to $\beta = \exp(-\pi) \simeq 0.043$ and $\Omega_{\rm th} = \pm 1$. In other words, the periodic states are expected here in the region of fairly small intensity ratio, see also Figure 2. For the parameters of SBN crystals [9] and $E_{\rm D} = 3$ kV/cm we estimate the minimum crystal thickness $x_{\rm th}^{\min} \approx 3$ mm. This means that the periodic states are available but can hardly be driven very far from the threshold.

The resonant response, $\theta = 0$, $0 < \cos\delta \ll 1$. In this case

$$\xi_{\rm th} = \frac{\pi^2 + \ln^2\beta}{\pi + \ln\beta\tan\delta}\,, \quad \Omega_{\rm th} = -\frac{\ln\beta}{\pi\cos\delta + \ln\beta\sin\delta}. \tag{9}$$

As a function of the intensity ratio, the dimensionless threshold thickness has a minimum at $\beta \simeq \exp(\pi\tan(\delta/2)) \gg 1$. Here we have

$$\xi_{\rm th}^{\min} = \frac{2\pi\cos\delta}{1+\cos\delta} = \frac{2\pi}{1+Q}. \tag{10}$$

Since $Q \gg 1$, it is considerably smaller than the minimum values of $\xi_{\rm th}^{\min}(\beta)$ found earlier for the local and nonlocal responses. For the sillenite parameters, with a DC-field $E_0 = 10$ kV/cm and $Q = 6$, we estimate $x_{\rm th} \approx 3$ mm. Thus the periodic states are also attainable here. The value

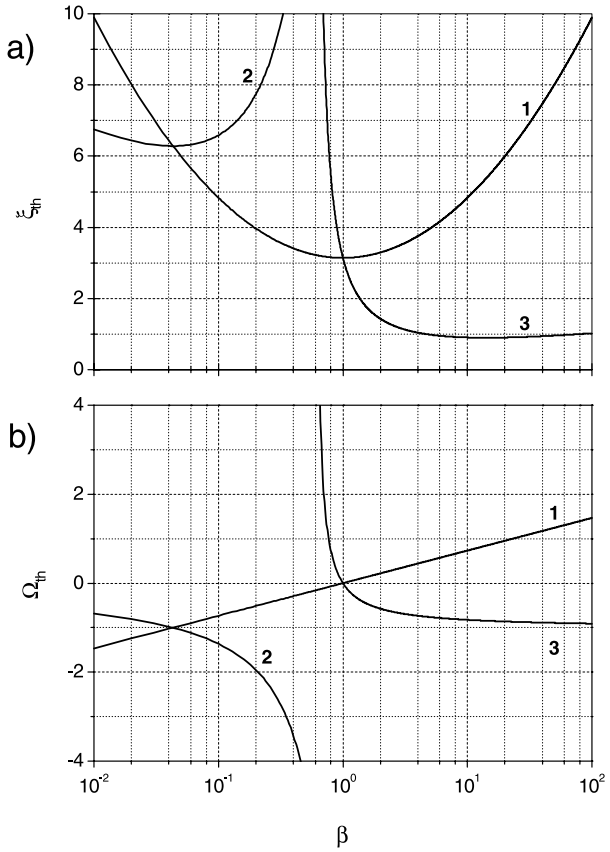

Fig. 2. Dependencies of the threshold thickness $\xi_{\rm th}$ and the threshold frequency detuning $\Omega_{\rm th}$ on the input intensity ratio β for the local (1), nonlocal (2), and resonant (3) nonlinear response. For curve 3 we have accepted $\delta = 80.4^\circ$, *i.e.*, $Q \simeq 6$.

of the frequency detuning at the threshold $\Omega_{\rm th} \approx -1$. Figures 2a and 2b illustrate the dependences $\xi_{\rm th}(\beta)$ and $\Omega_{\rm th}(\beta)$. Note a very slow growth of $\xi_{\rm th}(\beta)$ for the curve 3 after reaching the minimum.

The analysis performed in this section gives clear guidelines of where to search for the periodic states in the cases of local, nonlocal, and resonant nonlinear response.

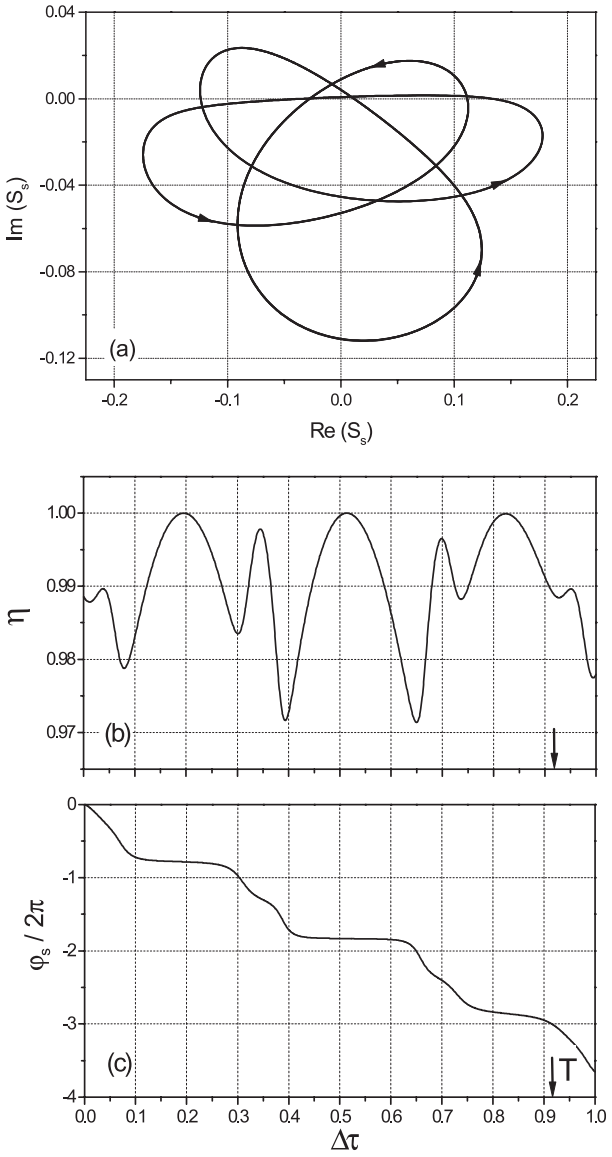

Fig. 3. The periodic state for the local response, $\xi_0 = 6$, $\beta = 1$, and $\tau_{\rm f}^{-1} = 10^3$: (a) the attractor trajectory of the amplitude $\mathcal{S}_s(\xi_0, \tau)$ on the complex plane; (b) the periodic time dependence of the diffraction efficiency η; (c) the time dependence of the input phase φ_s.

4 Periodic states

The case of the local response has been analyzed in detail in [7,8]. As a representative example we consider here the periodic state for $\beta = 1$ and $\xi_0 = 6 \simeq 1.9\,\xi_{\rm th}^{\rm min}$.

Figure 3a shows the trajectory $\mathcal{S}_s(\xi_0, \tau)$ on the complex plane during a time period of $T \simeq 0.92$. The amplitude $\mathcal{S}_s(\xi_0)$ describes the transmitted component of the unit S-beam testing the spatial grating [6,8]. To obtain the corresponding time dependencies, the set (1–4) was simulated with a zero initial condition for E up to $\tau \approx 50$, when the trajectory $\mathcal{S}_s(\xi_0, \tau)$ becomes strictly periodic. Because of the periodicity of the state, the behavior of the diffraction efficiency $\eta = |\mathcal{S}_s(\xi_0)|^2$ is shown in Figure 3b on a time interval longer than the period T. The corresponding time variable is denoted as $\Delta\tau$. One sees that during the whole period, η oscillates in the close vicinity of unity. Three revolutions around the zero-point occur during this time and the three apparent maxima of $\eta(\Delta\tau)$ correspond to the minimum distances of the trajectory from the origin. The input phase behavior is shown in Figure 3c. The dependence $\varphi_s(\Delta\tau)$ consists of a periodic part superimposed on a linear trend.

The value of the frequency detuning $\Omega_s = \langle\dot{\varphi}_s\rangle$ here is $\simeq -20.5$. At first sight, such a large value of Ω_s is surprising because one would expect that $|\Omega_s| \ll 1$ on the basis of the results of the previous section. It should be emphasized, however, that the dependence $\exp(\mathrm{i}\Omega_s\tau)$ becomes T-periodic when the product $\Omega_s T$ is an integer multiple of 2π. In other words, the linear trend of $\varphi_s(\Delta\tau)$ must

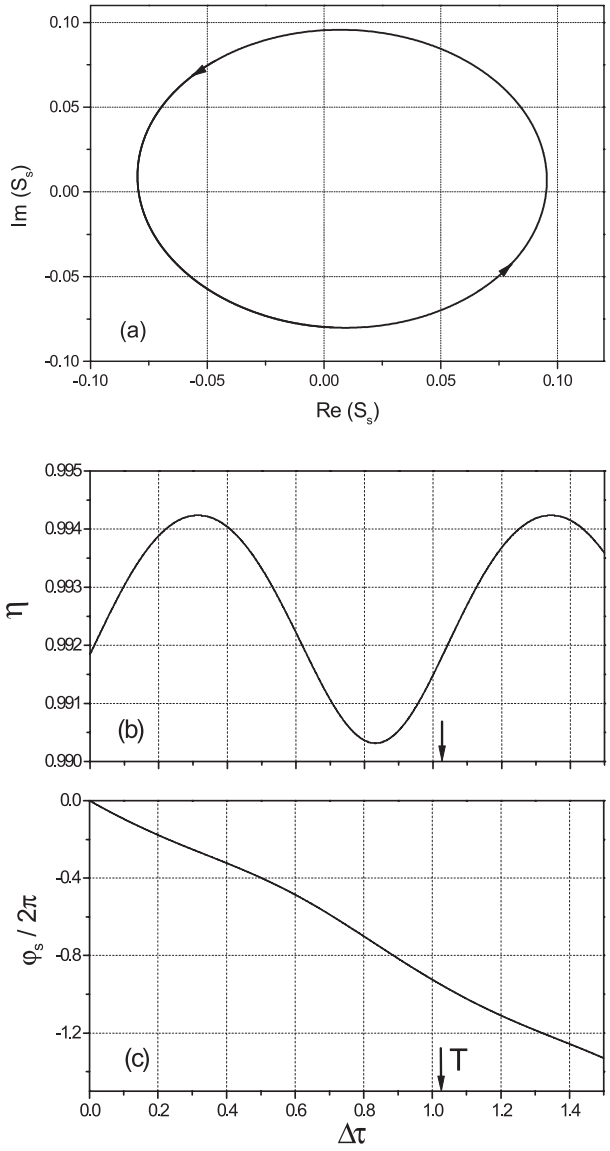

Fig. 4. The periodic state for the nonlocal response, $\xi_0 = 12$, $\beta = 1/23$, and $\tau_{\rm f}^{-1} = 10^3$: (a) the attractor trajectory of the amplitude $\mathcal{S}_s(\xi_0, \tau)$ on the complex plane; (b) the periodic time dependence of the diffraction efficiency η; (c) the time dependence of the input phase φ_s.

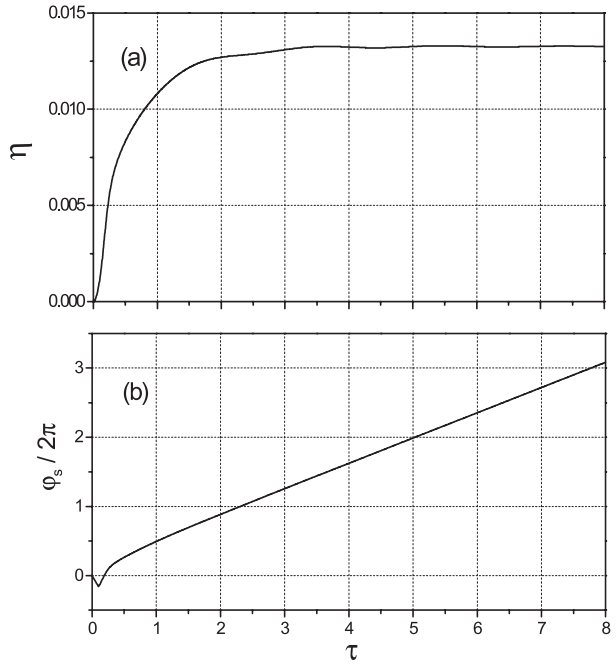

Fig. 5. Time dependencies of the diffraction efficiency η and the input phase φ_s for the resonant response, $\xi_0 = 1.5$, $\beta = 1/14$, $Q = 1/\cos\delta = 6$, and $\tau_{\rm f} = 10^{-3}$.

be treated here as a periodic phase modulation. One can check that $\Omega_s T \simeq -6\pi$ in our case.

Now we consider the case of the nonlocal response, $\delta = 0$, and $\theta = \pi/2$. With $\xi_0 = 12 \simeq 1.9\,\xi_{\rm th}^{\rm min}$ we were not able to find any periodic states for $\beta \sim 1$, which corresponds to the highest input contrast of the light interference pattern at the input. In this region, the system always approaches a steady state while η monotonously grows to a value which is considerably smaller than 1. The same is true for $\beta \gg 1$.

For the values of the pump ratio $\beta \approx 0.05$ we have managed, nevertheless, to find the expected periodic states. Figure 4a shows a representative example of an attractor. It has become settled after $\tau \gtrsim 50$ and consists of only one loop. Only one revolution around the origin occurs during a period of $T \simeq 1.03$. The distance to zero varies not very strongly with trajectory, in contrast to Figure 3a. The corresponding dependencies $\eta(\Delta\tau)$ and $\varphi_s(\Delta\tau)$ with a time $\Delta\tau$ varying from 0 to 1.5 are plotted in Figures 4b and 4c. Here the frequency detuning $\Omega_s \simeq -5.85$, and the difference $1 - \eta \lesssim 0.01$. The periodic component of the phase φ_s is here fairly weak.

With decreasing thickness ξ_0, the transient time increases dramatically and for $\xi_0 - \xi_{\rm th} \ll 1$ the periodic states become practically unattainable. This is similar in physics to the effect of critical slowing down known for many threshold (critical) phenomena.

Let us turn now to the case of the resonant response, which is expected to be the most interesting one. The distinctive features of this case can be detailed as follows. Basically, two characteristic times, 1 and $\cos\delta = Q^{-1} \ll 1$, are present on the left-hand side of equation (5). When far from the resonant steady-state with $\Omega \simeq 1$, the system develops with the characteristic time $\tau \sim 1$. At this stage the efficiency η is considerably less than unity. When the resonant state is approached, we can expect that Q becomes the proper unit to measure the dimensional time τ. At this stage, η can approach unity. We should also keep in mind that only large beam ratios, $\beta \simeq \exp[\pi \tan(\delta/2)] \gg 1$, are expected to be promising for the periodic states.

Figure 5 shows the dependences $\eta(\tau)$, and $\varphi_s(\tau)$ for $\xi_0 = 1.5$, $Q = 6$, and $\beta = 1/14$. One sees that after a fairly short time ($\tau \approx 4$) the system arrives at a steady state with moving light fringes, $\eta \simeq 0.013$, and $\Omega_s \simeq 2.3$. No periodic state occurs in this case.

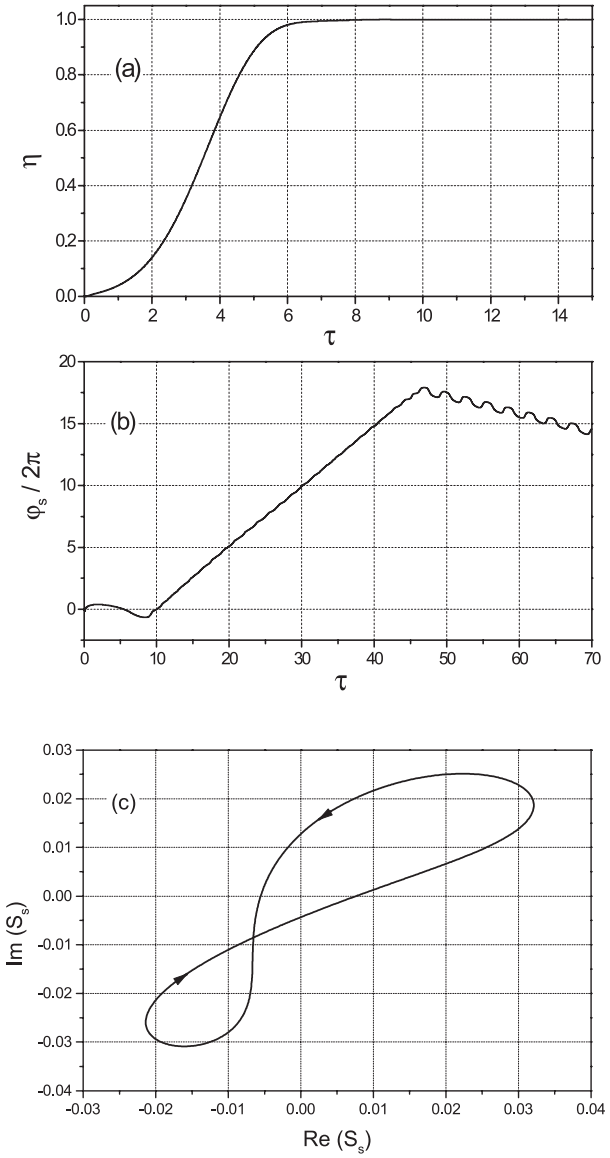

Fig. 6. Transient behavior and the periodic state for the resonant response, $\xi_0 = 1.5$, $\beta = 14$, $Q = 1/\cos\delta = 6$, and $\tau_\mathrm{f} = 10^{-3}$. The figures (a) and (b) show the initial stage of the time dependencies of the diffraction efficiency η and the input phase φ_s respectively. The plot (c) exhibits the attractor trajectory of the amplitude $\mathcal{S}_s(\xi_0, \tau)$ on the complex plane.

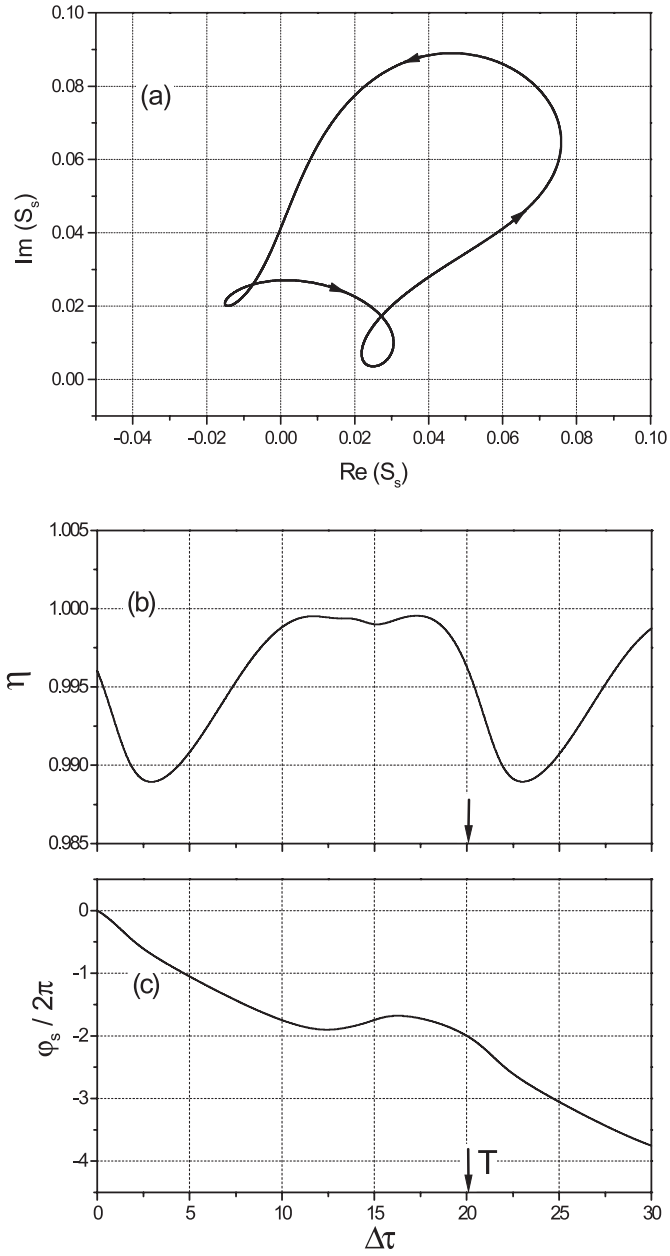

Fig. 7. The periodic state for the resonant response, $\xi_0 = 0.52$, $\delta = 85^\circ$, $\beta = 18$, and $\tau_\mathrm{f}^{-1} = 87$: (a) the $\mathcal{S}_s(\xi_0, \tau)$ attractor on the complex plane; (b) the periodic time dependence of the diffraction efficiency η; (c) the time dependence of the input phase φ_s.

The situation changes dramatically when we interchange the beam intensities, *i.e.*, reverse the intensity ratio, see Figure 6. The diffraction efficiency η rapidly approaches (at $\tau \approx 6$) unity and experiences then only very small oscillations. The phase behavior is more complicated. First, for $\tau \lesssim 9$ the input phase φ_s does not experience strong changes. Then (when η is already very close to unity) it starts to grow almost linearly. At $\tau \approx 47$ this growth switches abruptly to a linear decrease with clear periodic oscillations superimposed. No subsequent changes in this behavior are apparent. On the other hand, the trajectory becomes periodic only after a rather long evolution, $\tau \gtrsim 150$. It consists of two loops as shown in Figure 6c, the period $T \simeq 3.07$ and the phase slope for the periodic state is $\Omega_s \simeq -0.94$.

To see the main tendencies of the feedback system behavior we have decreased the value of $\cos\delta = Q^{-1}$, which characterizes the strength of the resonant response, to $\simeq 0.09$ ($\delta = 85^\circ$). The corresponding results for the periodic state are shown in Figures 7a–7c. The attractor consists now of three loops and it does not include the origin. The average tilt of $\varphi_s(\Delta\tau)$ is negative ($\Omega_s = -0.63$) and the period is much longer than previously, $T \simeq 20.1$. The diffraction efficiency oscillates between 0.99 and 1.

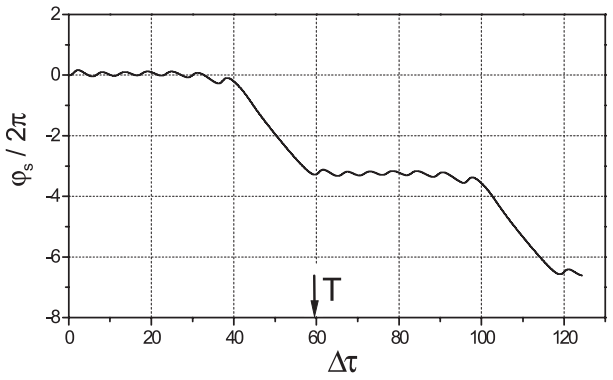

Fig. 8. Phase behavior for the periodic state in the case of the resonant response, $Q \simeq 19$, $\xi_0 = 0.4$, and $\beta = 19.7$. The period of the state $T \simeq 59.4$ and the average slope $\Omega_s \simeq -0.35$.

The transient time necessary to reach the periodic state is about 10^2. At the same time, the effective rise time (including the scaling factor of $\cos\delta \simeq 0.09$) is of the order of 10 and the product $T\cos\delta \simeq 1.8$ which is comparable with the corresponding figures for the previous case. Note that the feedback response time is chosen here to be relatively long, $\tau_{\rm f}^{-1} = 87$; this is in line with the assertion above regarding the increase ($\propto Q$) of the characteristic time of development in the vicinity of the periodic states.

Further decrease of $\cos\delta$ is accompanied by remarkable changes. The number of fine loops in the bottom of the trajectory is increased compared to Figure 7c. This peculiarity is accompanied by apparently two-periodic phase changes, see Figure 8 as an example. Each fine oscillation of $\varphi_s(\Delta\tau)$ corresponds to a small loop of the attractor. The total period T grows as $\approx 1/\cos\delta$ when δ approaches $\pi/2$.

5 Concluding remarks

The most important outcome of this study is that the feedback controlled periodic states are not restricted to the case of the local photorefractive response. Two other important cases, relevant to the nonlocal and resonant nonlinear response, are also promising for the feedback studies. Some basic features of the expected behavior, including the dependence on the beam ratio and the crystal thickness, obey rather general requirements deduced from the form of the existence curves.

The expected periodic behavior is distinguished by some new elements unknown in the case of the local response. These include peculiarities of the phase behavior for a strong resonant response and a relatively long period of oscillation. One can expect also a large diversity in the periodic and quasi-periodic regimes in this case.

To apply the scalar model of beam coupling to the case of the resonant response, it is necessary to avoid vectorial coupling effects typical of cubic crystals [14,15]. Crystals of BTO placed in a sufficiently large ($\gtrsim$ 7 kV/cm) DC-field parallel to the [001] axis offer probably the best possibilities for feedback experiments. With the input linear polarization perpendicular to [001] the scalar model used describes the wave amplitudes with a high accuracy.

The use of crystals possessing a nonlocal response like $BaTiO_3$ and SBN would also be of great interest because fully diffractive gratings cannot be obtained in this case in the standard frequency-degenerate experiments.

Financial support from the Deutsche Forschungsgemeinschaft is gratefully acknowledged.

References

1. A. Kamshilin, J. Frejlich, L. Cescato, Appl. Opt. **25**, 2375 (1986)
2. A. Freschi, J. Frejlich, J. Opt. Soc. Am. B **11**, 1837 (1994)
3. P.M. Garcia, K. Buse, D. Kip, J. Frejlich, Opt. Commun. **117**, 35 (1995)
4. P.M. Garcia, A.A. Freschi, J. Frejlich, E. Krätzig, Appl. Phys. B **63**, 207 (1996)
5. A. Freschi, P.M. Garcia, J. Frejlich, Opt. Commun. **143**, 257 (1997)
6. V.P. Kamenov, K.H. Ringhofer, B.I. Sturman, J. Frejlich, Phys. Rev. A **56**, R2541 (1997)
7. E.V. Podivilov, B.I. Sturman, S.G. Odoulov, S.L. Pavlyuk, K.V. Shcherbin, V.Ya. Gayvoronsky, K.H. Ringhofer, V.P. Kamenov, Opt. Commun. **192**, 399 (2001)
8. E.V. Podivilov, B.I. Sturman, S.G. Odoulov, S.L. Pavlyuk, K.V. Shcherbin, V.Ya. Gayvoronsky, K.H. Ringhofer, V.P. Kamenov, Phys. Rev. A **63**, 053805-1 (2001)
9. L. Solymar, D.J. Webb, A. Grunnet-Jepsen, *The Physics and Applications of Photorefractive Materials* (Clarendon Press, Oxford, 1996)
10. P. Refregier, L. Solymar, H. Rajbenbach, J.-P. Huignard, J. Appl. Phys. **58**, 45 (1985)
11. B.I. Sturman, M. Mann, J. Otten, K.H. Ringhofer, J. Opt. Soc. Am. B **10**, 1919 (1993)
12. J. Frejlich, P.M. Garcia, K.H. Ringhofer, E. Shamonina. J. Opt. Soc. Am. B **14**, 1741 (1997)
13. K.H. Ringhofer, V.P. Kamenov, B.I. Sturman, A.I. Chernykh, Phys. Rev. E **61**, 2029 (2000)
14. A. Marrakchi, R.V. Johnson, A.R. Tanguay, J. Opt. Soc. Am. B **3**, 321 (1986)
15. B.I. Sturman, E.V. Podivilov, K.H. Ringhofer, E. Shamonina, V.P. Kamenov, E. Nippolainen, V.V. Prokofiev, A.A. Kamshilin, Phys. Rev. E **60**, 3332 (1999)